International Conference on Applied Energy 2019
Aug 12-15, 2019, Västerås, Sweden
Paper ID: #376

OPTIMIZATION OF HYDRATE EXPLOITATION BASED ON HEAT TRANSFER ANALYSIS

Bo Li[1,2*], Shu Liu[1,2], Yun-Pei Liang[1,2], Qing-Cui Wan[1,2], Yong-Jiang Luo[1,2]

1 State Key Laboratory of Coal Mine Disaster Dynamics and Control, Chongqing University, Chongqing 400044, China

2 College of Resources and Safety Engineering, Chongqing University, Chongqing 400044, China

ABSTRACT

Hydrate decomposition is an endothermic reaction. The exploitation effect is closely related to the heat transfer properties in hydrate deposits. Based on the results of experiment and simulation with depressurization (PD), depressurization combined with wellbore heating (DH) and huff and puff method (HP), this paper mainly studies the heat transfer from the boundaries (Q_B), the heat consumption by hydrate decomposition (Q_H), the heat absorption by the porous sand (Q_S), and the heat loss (Q_L) to optimize the production methods. The results show that a limited amount of Q_L is caused by the heat transferred to the water bath in HP. In addition, the heat transferred from the water bath can offset the Q_S, which is the main component of Q_L in HP. Thus, the best heat utilization is seen in this method. PD shows its obvious weakness in hydrate recovery duration, although it only uses the Q_B for hydrate decomposition. For DH, the amount of the lost heat is the largest among the three methods, and the majority of Q_L is caused by the heat from wellbore heating transferred to the ambient environment. Thus, the heat utilization in this method is the worst. For the optimization of the exploitation method, it is of great importance to decrease the heat transferred to the surrounding environment.

Keywords: methane hydrate, huff and puff, wellbore heating, depressurization, heat transfer, heat utilization

1. INTRODUCTION

Natural gas hydrate is known as methane hydrate (MH), as it is formed by methane molecule and water under low temperature and high pressure. The abundant reserves of MH in ocean and permafrost make it an alternative energy resource in the future (about 2.0×10^{16} m^3 of methane gas under standard conditions) [1, 2]. At present, the feasible production methods include pure depressurization [3], pure heating [4], combination method [5], inhibitor injection [6] and displacement method [7]. The widely used methods should be pure depressurization (PD) and depressurization combined with heating method (DH), in which the huff and puff method (HP) is a special DH method with discontinuous heating. However, it is difficult to exploit MH with high energy efficiency under severe occurrence conditions. This is because MH dissociation is an endothermic process that requires heat from surrounding environments. So many researches about heat transfer during hydrate dissociation have been carried out.

Zhao et al. [8] conducted numerical simulation to study the effect of heat transfer on MH dissociation with depressurization. They found that heat transfer was impacted by the material of hydrate deposit and the water contained in the pores. Ji et al. [9] used a one-dimensional linearized model to investigate the gas production behavior by depressurization. The results showed that gas production was easily influenced by production pressure, sediment temperature and deposit permeability. Oyama et al. [10] presented a decomposition model which is a function of heat and mass transfer. By comparing the results of this model and experiment in depressurization, they verified the predictability of the dissociation model and concluded that the heat transfer from the surrounding environment dominated the hydrate exploitation.

From the studies of PD, one can see that the insufficient heat transfer from the ambient environment inhibits hydrate exploitation. Thus, adding extra heat in production needs to be considered. By the comparison of the results of experiments with that of numerical simulations, Wan et al. [11] studied the heat transfer behaviors in a 3D cubic vessel. They thought

Selection and peer-review under responsibility of the scientific committee of the 11th Int. Conf. on Applied Energy (ICAE2019).

that the driving forces of depressurization and heating dominated the hydrate decomposition. Li et al. [12] carried out the hydrate decomposition experiment in the 3D cubic hydrate simulator using HP method. The results indicated that the higher injection temperature and longer injection duration might not improve the thermal efficiency and energy efficiency. After conducting experimental study in a Cuboid Pressure Vessel, Li et al. [13] drew the conclusion that electrical heat injection had the ability to greatly improve the production efficiency of depressurization. Liang et al. [4] mainly analyzed exploitation time and energy efficiency for comparing the production effects of PD, HP with DH. The results indicated that a better exploitation could be achieved in DH method with a reasonable heating power, and HP method was the best for commercial exploitation.

One can see that the majority of papers about the evaluation of production effects of different exploitation methods are based on the analysis of parameters including gas production, net energy gain and energy efficiency. Although an increasing number of studies focus on the analysis of heat transfer during exploitation process, few researchers have quantitatively studied the heat transfer processes of different exploitation methods, not to mention the analysis of heat transfer for the optimization of production methods. Based on the results of three experimental runs with different exploitation methods (i.e., PH, DH and HP) conducted in the Cuboid Pressure Vessel (CPV), this paper quantitatively investigates the heat transfer from the CPV boundaries (Q_B), the heat consumption by hydrate decomposition (Q_H), the heat absorption by the porous sand (Q_S), and the heat loss (Q_L) during decomposition process by numerical simulation. The TOUGH+HYDRATE (T+H) code is employed for the numerical study.

2. EXPERIMENT AND SIMULATION

2.1 Experimental device

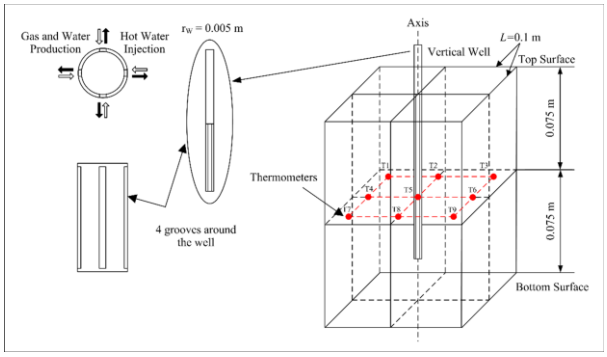

Fig 1 Cuboid Pressure Vessel internal structure and well design

The experimental device is mainly formed with temperature system, gas supply system, fluid system, gas-liquid separation system and data acquisition system. MH formation and decomposition are carried out in the Cuboid Pressure Vessel (CPV) with the volume of 1.5 L (length × width × height: 100 × 100 × 150 mm), as shown in Fig. 1. A vertical well is located in the center of the CPV with the length of 120 mm and the diameter of 10 mm.

Nine thermometers (i.e., T1 - T9) are distributed in the central horizontal plane of CPV for the measurement of temperature change in the CPV. T5 is placed in the center of the CPV, and T1, T3, T7 and T9 are located in four corners of the CPV respectively. Others are placed in the boundary center. In each boundary, the distance between one corner thermometer and one boundary center thermometer is 40 mm. A resistance-heating rod (73.5 Ω) is placed in the vertical well. The gas and water production and wellbore heating are carried out through four grooves on the surface of the vertical well.

2.2 *Experimental and numerical simulation procedure*

2.2.1 Experimental procedure

After filled with quartz sand with the particle size of 0.27 - 0.38 mm, the porosity of the MH sediment was tested to be 44.2%. Then 3.30 mol of methane gas and 370.23 mL of deionized water were injected into the CPV, and the pressure in the CPV increased to about 22.0 MPa. The temperature of the water bath kept stable at 7.8 ^{o}C. When the pressure of the CPV decreased to 8.0 MPa, the hydrate formation process ceased.

There were two stages in the hydrate decomposition process. The stage I was the free gas and mix gas release stage. When the pressure dropped to the target exploitation pressure (P_W = 5.0 MPa), the stage II began. This paper studied the production behavior during the stage II due to the constant P_W and no free gas production. For PD, the P_W was kept at 5.0 MPa. For DH, when this stage began, the wellbore heating started. For HP, the stage II consisted of several cycles. Each cycle consists of the heating step for 5 min, the soaking step for 3 min and the production step. The CPV was closed in the former two cycles and it kept opened in the production step. One can find more detailed information about this experimental device and operation procedures in the published papers [6, 9, 10].

2.2.2 Numerical simulation procedure

The three-dimensional grid used by Wan et al. [11] is employed in the numerical simulation section. The three phase saturations are initialized to be S_{H00}, S_{L00}, and S_{G00} listed in Table 1. The initial pressure is set to be equal to the production pressure P_W, and the initial temperature is calculated according to the methane hydrate P-T equilibrium model in the TOUGH+HYDRATE code. The detailed mass, energy, and momentum balance equations as well as other related models can be found in the employed code. The boundary temperature is set to be 7.8 °C. For the PD and DH cases, the pressure of the grid representing the vertical well is maintained to be P_W, and the heat injection rate is set to be 0 and 25 W, respectively. For the HP case, the heat injection rate of the wellbore grid is set to be 25, 0, and 0 W in the injection, soaking and production steps, respectively, and the pressure of the wellbore grid is only maintained constant at P_W in the production step. The various heat flows, including the heat transfer from the CPV boundaries (Q_B), the heat consumption by hydrate decomposition (Q_H), the heat absorption by the porous sand (Q_S), and the heat loss (Q_L), are monitored and calculated using the calculation methods of Wan et al. [11] during the numerical simulations.

Table 1. Summary of the experimental parameters and numerical simulation results for the three runs

Run	Method	S_{H00}	S_{L00}	S_{G00}	Q_W(W)	P_W(MPa)	V_P(L)	Δt(min)	Q_B(KJ)	Q_S(KJ)	Q_L(KJ)
1	PD	0.302	0.320	0.378	0	5.0	31.98	427.5	81.7	4.8	4.8
2	DH	0.295	0.323	0.382	25	5.0	30.07	93.9	-39.4	26.4	65.8
3	HP	0.314	0.258	0.428	25	5.0	31.98	113.4	-2.5	15.0	17.5

where, run 1, 2 and 3 represent experimental group 1, 2 and 3, respectively; HP (huff and puff method), DH (depressurization combined with wellbore heating) and PD (pure depressurization) stand for the exploitation method in run 1, 2 and 3, respectively; S_{H00}, S_{L00} and S_{G00} stand for the initial saturation of the hydrate, the liquid and the gas at the beginning of the stage II, respectively; Q_B, Q_S and Q_L are the heat flowing across the boundaries, the heat absorption by the porous sand and the heat loss respectively at the end of the production in simulation; P_W, V_P and Δt represent the production pressure, the accumulative gas production and the exploitation duration, respectively.

3. RESULTS AND DISCUSSION

3.1 Gas production

Fig. 2 shows gas production of three runs in experiment and simulation, respectively. The V_P of experiment and simulation corresponded well in each run. This indicated the reliability of the simulation [17, 21, 22]. The run with PD showed the obviously longest production duration of 427.5 min. The extra heat injection could greatly enhance the production effect in runs with DH and HP. With the same heating rate and production pressure, the production duration of HP was a little longer than that of DH. The gas production behaviors were closely related to the different heat transfer characteristics with distinct exploitation methods of PD, DH and HP. So, we should quantitatively consider the heat transfer aspect for analyzing the production effect of three runs.

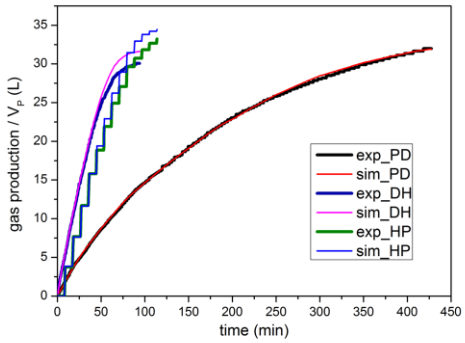

Fig 2 Gas production of three runs. exp_PD, exp_DH and exp_HP represent V_P in experiments by pure depressurization, depressurization combined with heating and huff and puff method, respectively. sim_PD, sim_DH and sim_HP stand for V_P in simulation by PD, DH and HP, respectively.

3.2 Heat transfer analysis

3.2.1 Heat transfer from boundaries and heat absorption for MH decomposition

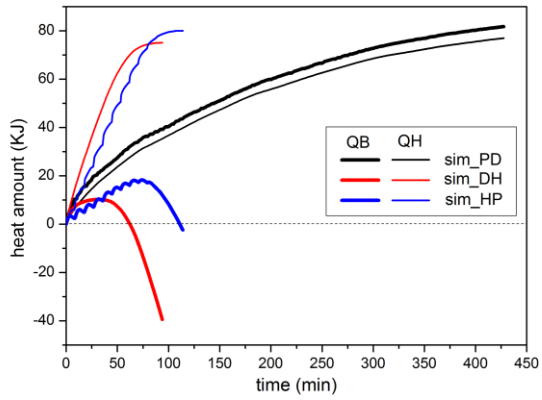

Fig 3 Heat transfer from CPV boundaries (Q_B) and heat absorption by hydrate decomposition (Q_H) with PD, DH and HP in numerical simulation.

Fig. 3 illustrates heat transfer from boundaries (Q_B) and heat absorption by hydrate decomposition (Q_H) in three runs. Hydrate decomposition is an endothermic reaction, so Q_H in three runs showed an increasing trend with time. Due to the only driving force of depressurization, the heat absorption rate with PD was the slowest. The heat absorption rate of DH was higher than that of HP during almost entire production time. But just rising to the peak value of 10.0 KJ in the early decomposition period, the Q_B of DH dropped far below 0 KJ (– 39.4 KJ). This indicated that a lot of heat was transferred to the water bath as heat loss in this run. The Q_B of HP increased to about 20.0 KJ before it decreased just below 0 KJ at the end of the hydrate dissociation. This showed us that during almost the entire exploitation, the heat from the water bath was transferred to the CPV rather than that the heat in the CPV was transferred to the ambient environment to lead to a lot of heat loss. It owed to the discontinuous heating [4]. So the run with HP showed better advantage in utilizing the heat transfer from the surrounding environment than that with DH. The run with PD was the only run that the Q_B showed a gradual rising trend during the whole decomposition time. This was because the only driving force for hydrate decomposition was the continuous heat transfer from the water bath.

From the above analysis, one could see that although the Q_B increased positively with PD, there was a gap between the Q_B and Q_H. It indicated that there was heat loss absorbed by the hydrate sediment even with PD. So, we need to consider the heat loss.

3.2.2 Heat loss and sensible heat of hydrate sediment

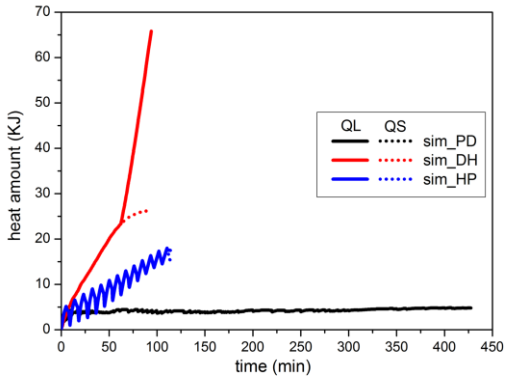

Fig 4 Heat loss (Q_L) and sensible heat of hydrate sediment (Q_S) with PD, DH and HP.

Fig. 4 illustrates the heat loss and sensible heat of the hydrate sediment of three runs. In this study, the effect of water and gas on heat loss is neglected due to the limited amount of water production and the relatively low specific heat capacity of gas [6, 17]. In the runs with DH and HP, the heat loss consisted of two aspects of heat transfer from boundaries (Q_B) and the heat absorption by the hydrate sediment (Q_S). When $Q_B < 0$, it can be calculated as: $Q_L = Q_S - Q_B$, KJ; if $Q_B > 0$, it is shown as: $Q_L = Q_S$, KJ. For PD, only the heat absorption by the hydrate sediment was regarded as the heat loss. So the Q_L and Q_S of PD corresponded with each other.

With PD, the Q_L and Q_S increased moderately from 0 to only 4.8 KJ. Other two runs showed obviously larger Q_L and Q_S than that with PD. In HP, the Q_L corresponded with Q_S during almost the entire production time. This showed us that almost all the heat loss was used to improve the sensible heat of the hydrate sediment.

The largest heat loss was seen in DH. With the same heating rate and production pressure, the final Q_L and Q_S were almost four times and twice as large as those with HP, respectively, as shown in Table 1. Due to a large amount of heat transferred to the water bath, this run showed a worse decomposition effect in heat utilization. It explained the low energy efficiency in DH according to the aspect of heat utilization.

4. CONCLUSIONS

In HP method, majority of the heat loss was caused by the heat consumption of the hydrate sediment. The heat transferred from the water bath into the CPV is

enough to provide the heat absorption by the porous sand. Thus, the obvious advantage was seen in heat utilization with this method.

Although the hydrate only absorbs the heat transferred from the ambient environment for decomposition in PD, it shows obvious weakness in production duration. In addition, the heat transferred from the surrounding environment is excessive, and part of heat is absorbed by the porous sand as the heat loss.

In DH, the low energy efficiency is caused by a lot of heat transferred to the ambient environment. It shows little advantage in heat utilization.

For the optimization of exploitation method, it is vital to avoid the added heat to be transferred to the water bath. Furthermore, one can think about the utilization of the heat transferred from the ambient environment to obtain higher energy efficiency.

ACKNOWLEDGEMENT

This work is supported by the National Natural Science Foundation of China (51876017 and 51506016) and the Chongqing Foundation and Advanced Research Project (cstc2016jcyjA0034), which are gratefully acknowledged.

REFERENCE

[1] Jr EDS, Koh CA. Clathrate Hydrates of Natural Gases. Crc Press. 2007.

[2] Feng JC, Wang Y, Li XS, Li G, Zhang Y, Chen ZY. Effect of horizontal and vertical well patterns on methane hydrate dissociation behaviors in pilot-scale hydrate simulator. Appl. Energy 2015;145:69-79.

[3] Haligva C, Linga P, Ripmeester JA, Englezos P. Recovery of Methane from a Variable-Volume Bed of Silica Sand/Hydrate by Depressurization. Energy Fuels 2010;24:2947-55.

[4] Liang YP, Liu S, Wan QC, Li B, Liu H, Han X. Comparison and Optimization of Methane Hydrate Production Process Using Different Methods in a Single Vertical Well. Energies 2018;12:1-21.

[5] Falser S, Uchida S, Palmer AC, Soga K, Tan TS. Increased Gas Production from Hydrates by Combining Depressurization with Heating of the Wellbore. Energy Fuels 2012;26:6259-67.

[6] Kawamura T, Sakamoto Y, Ohtake M, Yamamoto Y, Haneda H, Yoon JH, et al. Dissociation Behavior of Hydrate Core Sample Using Thermodynamic Inhibitor. Int. J. Offshore Polar Eng. 2006;16:5-9.

[7] Komatsu H, Ota M, Jr RLS, Inomata H. Review of CO2–CH4 clathrate hydrate replacement reaction laboratory studies – Properties and kinetics. J. Taiwan Inst. Chem. Eng. 2013;44:517-37.

[8] Zhao J, Liu D, Yang M, Song Y. Analysis of heat transfer effects on gas production from methane hydrate by depressurization. Int. J. Heat Mass Transfer 2014;77:529-41.

[9] Ji C, Ahmadi G, Smith DH. Natural gas production from hydrate decomposition by depressurization. Chem. Eng. Sci. 2001;56:5801-14.

[10] Oyama H, Konno Y, Masuda Y, Narita H. Dependence of Depressurization-Induced Dissociation of Methane Hydrate Bearing Laboratory Cores on Heat Transfer. Energy Fuels 2009;23:4995-5002.

[11] Wan QC, Si H, Li B, Li G. Heat transfer analysis of methane hydrate dissociation by depressurization and thermal stimulation. Int. J. Heat Mass Transfer 2018;127:206-17.

[12] Li XS, Wang Y, Duan LP, Li G, Zhang Y, Huang NS, et al. Experimental investigation into methane hydrate production during three-dimensional thermal huff and puff. Appl. Energy 2012;94:48-57.

[13] Li B, Liu SD, Liang YP, Liu H. The use of electrical heating for the enhancement of gas recovery from methane hydrate in porous media. Appl. Energy 2018;227:694-702.

[14] Liang YP, Liu S, Zhao WT, Li B, Wan QC, Li G. Effects of vertical center well and side well on hydrate exploitation by depressurization and combination method with wellbore heating. J. Nat. Gas Sci. Eng. 2018;55:154-64.

[15] Li B, Liang YP, Li XS, Wu HJ. Numerical analysis of methane hydrate decomposition experiments by depressurization around freezing point in porous media. Fuel 2015;159:925-34.

[16] Li B, Liang YP, Li XS, Zhou L. A pilot-scale study of gas production from hydrate deposits with two-spot horizontal well system. Appl. Energy 2016;176:12-21.